9 Lithography with Self-Assembled Block Copolymer Microdomains

CHRISTOPHER HARRISON
Schulumberger-Doll Research, 36 Old Quarry Road, Ridgefield CT 06877, USA

JOHN A. DAGATA
National Institute of Standards and Technology, Gaithersburg MD 20899, USA

DOUGLAS H. ADAMSON
Princeton Materials Institute, Princeton University, Princeton NJ 08540, USA

9.1 INTRODUCTION

9.1.1 MOTIVATION

The quest for faster, cheaper, and more powerful electronics has driven the semiconductor industry to ever smaller feature sizes, ca. 130 nm at the time of writing. The ingenuity and success of this industry are breathtaking [1]. As the expense of lithographic technologies has increased and the importance of computational power has grown, alternatives to conventional photolithography have been put forward by academic and industrial researchers. One such alternative, the focus of this review, has been the use of block-copolymer microdomains as a lithographic template. Rather than using photolithography or electron beam lithography as a means of pattern formation, a block copolymer is allowed to self-assemble into the desired structure. Some degree of intelligent guidance may be utilized, depending upon the application's needs. While self-assembly is generally limited to a few periodic forms of high symmetry (e.g. spheres or cylinders), it turns out that there is great use for such structures in lithography, particularly that related to information storage.

There are many research groups working on block-copolymer lithography; many more have expressed interest in joining the field. Researchers who are new to this area will find the broad review of block copolymer thin films by Fasolka and Mayes [2] to be a highly valuable resource. However, to this researcher's knowledge, no comprehensive review of block copolymer lithography currently exists. Therefore, we undertake one such review here that will enable lithography researchers to quickly come up to speed.

Developments in Block Copolymer Science and Technology. Edited by I. W. Hamley
 ISBN: 0–470–84335–7

9.1.2 ANECDOTAL ORIGIN OF BLOCK COPOLYMER LITHOGRAPHY

According to the often-told story, sometime in the late 1980s, P. M. Chaikin was in the office of L. J. Fetters at Exxon Research and Engineering where he noticed an electron micrograph of a hexagonal array of dots [3]. The array was produced by a microphase-separated block copolymer system with a lattice spacing of 30 nm. Realizing that this length scale was perfect for electron transport measurements of the so-called Hofstadter butterfly pattern [4], he began research to harness these patterns as lithographic templates, first putting P. Mansky on the task [5]. With the help of N. Thomas's students, they were able to show that polystyrene-polyisoprene block copolymers were largely compatible with semiconductor-based lithographic techniques. The addition of R. A. Register brought further copolymer expertise to the project, especially concerning the use of ozone for templating nanostructures, the focus of one of us (C. H.) during his first years in graduate school. Progress was further facilitated with the synthesis of a wide range of block copolymers by one (D. H. A.) of us. The project accelerated with the addition of Miri Park whose nanolithography skills had been honed at the Cornell Nanofabrication Facility. Indeed, the majority of the initial publications resulted from numerous trips from Princeton to Ithaca, a perilous journey during the winter. Subsequent group members continued to develop the technology such that the polymer pattern could be transferred to semiconductor and metallic films. Since then many research groups have joined the field and prototypes of products based on this technology are being evaluated.

9.1.3 EMERGING TECHNOLOGY

A further motivation to writing this chapter has been the use of copolymer lithography by researchers at the Corporate Research and Development Center of the Toshiba Corporation. Section 9.7 [6] details their clever use of copolymer lithography for information storage. These researchers demonstrate that CoCrPt films can be patterned without difficulty on hard-drive platters that have been embossed for microdomain templating. While applications such as this were one of the motivations for academic work over the past decade, until recently there has been a paucity of projects with a truly applied focus.

9.1.4 OVERVIEW OF CHAPTER

We present an overview of this chapter's organizational layout. In Section 9.2 we describe polymer synthesis and the resulting self-assembled structures, both in bulk and thin films. In Section 9.3 we describe the imaging technologies

necessary for working in this field. Building on this, we describe the means to control microdomain orientation in Section 9.4. Section 9.5 discusses the chemical and metallic modifications that are possible to optimize a copolymer pattern for lithographic use. Section 9.6 describes the progress of researchers applying conventional lithographic tools to copolymer templates. Finally, Section 9.7 discusses currently emerging applications and possibilities for the future.

9.2 SELF-ASSEMBLED STRUCTURES

Self-assembly is a smart means of using chemistry and thermodynamics to select a desired pattern. While self-assembly can be used in a variety of systems ranging from surfactant-templated silicates [7] (nanometers) to colloidal dispersions (microns) [8], the focus here will be on block copolymers (tens of nanometers). Block copolymers with $\chi N \gg 10$ microphase separate above their glass transition temperature, where χ is the Flory–Huggins interaction parameter and N is the degree of polymerization [9,10]. The resulting morphology depends largely on the relative volume fraction of the components. Some of the more commonly seen morphologies are lamellae, cylinders, and spheres (Figure 9.1). The length scale of microdomains is determined by the length of the polymer

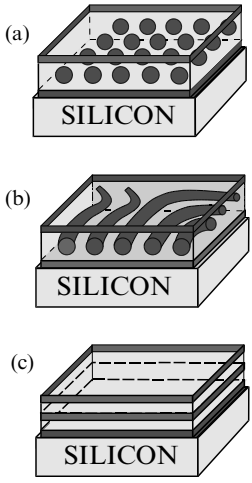

Figure 9.1 Schematic of block-copolymer microdomains in thin films. Panels a and b show one layer of spheres and cylinders, respectively (darker component). Note the additional wetting layers above and below the microdomains that serve to satisfy the interfacial constraints; the specific configuration varies depending upon the copolymer system. Panel c shows lamellar sheets oriented parallel to the substrate by the strong alignment influence of the substrate and vacuum/polymer interfaces. (Reproduced with permission from the American Association for the Advancement of Science)

chains. The thermodynamics of these structures have been extensively examined in bulk, and more recently, in thin films [2].

9.2.1 CHEMICAL SYNTHESIS

The narrow polydispersity of block copolymers (necessary for self-assembly with a good degree of long-range order) is greatly facilitated by the use of living anionic polymerization techniques [11–13]. Anionic polymerization affords a fairly large selection of monomers and yields materials with well-defined composition and well-controlled molecular mass. Due to these advantages, anionic polymerization is the typical method used in the synthesis of polymers for self-assembly. Recently, however, some evidence has emerged that certain polydisperse systems microphase separate to produce periodic structures with good order [14].

Nonpolar hydrocarbon monomers such as styrene, isoprene, and butadiene are polymerized in hydrocarbon solvents such as benzene or cyclohexane. Initiation is achieved with the use of alkyllithiums such as sec-butyllithium and molecular mass is controlled by the ratio of initiator to monomer. The living nature of anionic polymerization allows the syntheses of block copolymers by sequential addition of the monomers. After one monomer is exhausted, the chain remains reactive, or "living." The addition of the second monomer then continues the polymerization to form a block copolymer. Such techniques are used to synthesize polystyrene-polyisoprene or polystyrene-polybutadiene copolymers (PS-PI or PS-PB, respectively).

Polar monomers such as 2-vinylpyridine and methyl methacrylate are normally polymerized in polar solvents such as tetrahydrofuran and at low temperature ($-78\,^{\circ}C$). In addition, additives such as LiCl are often added to help lower the rates of termination reactions to levels insignificant in the time frame of the reaction. Block copolymers made with nonpolar and polar monomers start with the nonpolar monomer because of its greater reactivity. These active centers are then typically capped with 1,1-diphenylethylene to lower their reactivity before the addition of the polar monomer. This helps eliminate side reactions resulting from addition of the active center to electrophilic sites in the polar monomers. The two polar polymers, polystyrene-2-vinylpyridine (PS-P2VP) and polystyrene-poly methyl methacrylate (PS-PMMA) have been extensively studied in thin films.

Ring-opening anionic polymerization is used in the synthesis of polyferrocenyldimethylsilane (PFS) (see section 9.6.3). This mechanism involves nucleophilic addition of a polymer anion to a cyclic monomer. The monomer then ring opens, leading to incorporation of the monomer into the growing chain and generation of a new anion. This method is not as common as those previously mentioned, but can result in well-defined polymers with unique chemical composition.

Experimentally, there are two general methods for anionic polymerization. One is high-vacuum polymerization, and the other is inert-atmosphere polymerization. High-vacuum polymerization has the advantage of higher levels of purity over longer periods of time. This can be very important for high molecular mass polymers or polymers containing coupling agents that have long reaction times (months) and must be kept very clean for a long time. The disadvantage is the added effort and time needed to run a reaction under high vacuum. The reactor must be made with glass-blowing techniques and the reactants added by break seals.

Inert-atmosphere techniques, on the other hand, are complementary to high-vacuum techniques. Rather than using a vacuum, an inert gas such as nitrogen or argon is used to maintain the absence of moisture, oxygen or carbon dioxide. Less effort is required, and for simple diblock copolymers, the loss of some purity may not be detrimental to the self-assembly of the polymers.

A relatively new technique used for the random PI-PS brushes mentioned later in this review (Section 9.2.2) is controlled-radical polymerization [15–17]. This technique reduces the rate of radical recombination by lowering the effective concentration of radicals. This new method opens the possibility of random polymers such as those used in brushes. These polymers have a relatively narrow polydispersity (especially for radically produced polymers).

Hydrogenation is often used to improve the chemical and thermal stability of polymers. Hydrogenation of isoprene, for instance, saturates the double bonds to form poly(ethylene propylene) or PEP [18]. This polymer is chemically distinct from PI and has different properties. One advantage is that PEP is much less sensitive to oxidation than PI, and so can be heated in the presence of oxygen with no significant degradation. Hydrogenation is done under hydrogen pressure, with either soluble or insoluble catalysts. It is possible to hydrogenate a diene in the presence of styrene, or to hydrogenate the styrene as well.

9.2.2 SELF-ASSEMBLY IN THIN FILMS

While bulk systems are easier to analyze, effective and rapid implementation of copolymer lithography is contingent upon the fabrication and control of microdomains in resist-like thin films. Use of such films can take advantage of well-developed resist technologies (spin coating and film characterization) thereby speeding their adaption into fabrication environments. However, the structure formed by copolymers in bulk or melt state may differ from that of thin films. Such films can easily be fabricated by spin coating from dilute (ca. 1% wt) solutions onto smooth silicon wafers where the thickness can be easily tuned by the usual parameters of spin speed and solution concentration. For films of thickness comparable to the microdomain spacing (10 nm to 100 nm thick), the influence of the interface dominates, leading to structures different from that in bulk. A large fraction of polymer in thin films is devoted to satisfying the

wetting constraints, e.g. PMMA preferably wets silicon wafers in a PS-PMMA system [2]. Microdomains are often submerged inside the film, though this depth depends upon the molecular mass and chemistry of the copolymer system [18]. Films thinner than a critical thickness often exhibit no microdomains as all polymeric material is used to wet the interfaces. Microdomain structure varies as well – many researchers have noted that copolymers that form cylinders in bulk form spheres in sufficiently thin films [19]. Lastly, thin films often suffer from kinetic or pinning influences from the surface that lead to short microdomain correlation lengths or grain sizes. Surface modifications have been employed to try to ameliorate surface pinning [20].

9.3 IMAGING MICRODOMAINS IN THIN FILMS

Perhaps the first challenge faced by researchers working on copolymer lithography was finding a fast, reliable, and robust imaging technique. Rigorous diagnosis of the success or failure of each lithography step requires analysis via an imaging method; since there can be dozens of steps in multilayer lithography a rapid technique is essential. There are two dominant imaging techniques that have emerged as strong research tools: the scanning electron microscope (SEM) and the atomic force microscope (AFM). The instrument choice depends mainly upon which technique generates higher contrast for each particular copolymer system, and of course, availability and researcher preference.

9.3.1 ELECTRON MICROSCOPY

The earliest work on imaging block copolymer microdomains relied heavily upon transmission electron microscopy (TEM), and it still proves to be a useful tool to this day [19]. Samples are either microtomed or solvent cast to produce thin (ca. 100 nm) sections. PS-PI or PS-PB samples can be stained with osmium tetroxide to increase contrast. Osmium tetroxide reacts selectively with unsaturated double bonds such as found in PI or PB microdomains so as to provide mass contrast [21]. Unfortunately, TEM requires that the samples be freestanding or transferred to a transparent support (e.g. carbon), a cumbersome and time-consuming process that is largely incompatible with silicon or GaAs wafers. While silicon nitride membranes can be employed for TEM, these expensive and delicate structures are not easily accessible to all researchers [22].

Compared to TEM, scanning electron microscopy (SEM) suffers from lower resolution but its ease of use and ability to image surface features have made it the workhorse of microlithography. Indeed, easy access to SEMs in clean-room environments plays a large role in its choice by many researchers. Furthermore, developments in the past decade have made low-voltage, high-resolution

SEM more commonplace in clean rooms, narrowing the resolution gap between SEM and TEM [23]. Low-voltage SEM (around 1 kV) is advantageous for the insulating nature of copolymer masks increases its susceptibility to charging effects. In some cases, a thin metal coating is used to decrease sample charging, but researchers often find this unnecessary when using the latest generation of low-voltage scanning electron microscopes–an advantage not be overlooked, as coating a sample with a nonuniform metal film can obscure important features. Examples of SEM micrographs of spherical and cylindrical microdomains are shown in Figure 9.2

Microdomains that present surface topography, such as those formed by PS-PMMA copolymers, are readily imaged by SEM with standard topography enhancing operating procedures. However, microdomains of other copolymer systems such as PS-PI are often submerged beneath a surface wetting layer, requiring additional steps to enhance contrast. First, conventional OsO_4 staining is used to produce contrast in a manner consistent with TEM sample preparation. In some cases, the operating voltage can be used to image slightly submerged microdomains. Specifically, low-voltage (1 kV) SEM enhances features within the top 10 nm, but by increasing the operating voltage to 5 kV, features as deep as 25 nm have been successfully imaged [24]. Secondly, for those features further submerged beneath the surface, reactive ion etching has been shown to provide an even higher level of contrast; optimal choice of the etching gas to minimize (or maximize) the selectivity is paramount [18]. Plasma etching has the added advantage of providing depth information, important in multilayer systems [25].

9.3.2 ATOMIC FORCE MICROSCOPY

Atomic force microscopy has become a powerful tool for examining the surface of block copolymer films. Researchers have produced a set of publications on imaging copolymer microdomains and proved its utility in many, though not all, copolymer systems [26–29]. Unfortunately, AFMs are often not readily available in the typical clean-room setting, though their presence is growing. Additionally, an inexperienced researcher can easily damage the AFM tip, the recognition of which is a learned skill and leads to a very shallow learning curve.

An AFM generates contrast by sensing either topographic features or variation in mechanical properties, the latter by measuring the phase of an oscillating tip. Tapping mode appears to be the preferred imaging method as indicated by the frequency of publications that describe its use in imaging polymer films. For PS-PMMA copolymer systems, Morkved and coworkers [22] have argued that contrast originates from purely topographic effects, which is plausible as the moduli of PS and PMMA are virtually identical over a wide range of temperatures. Alternatively, a modulus difference between microdomains and

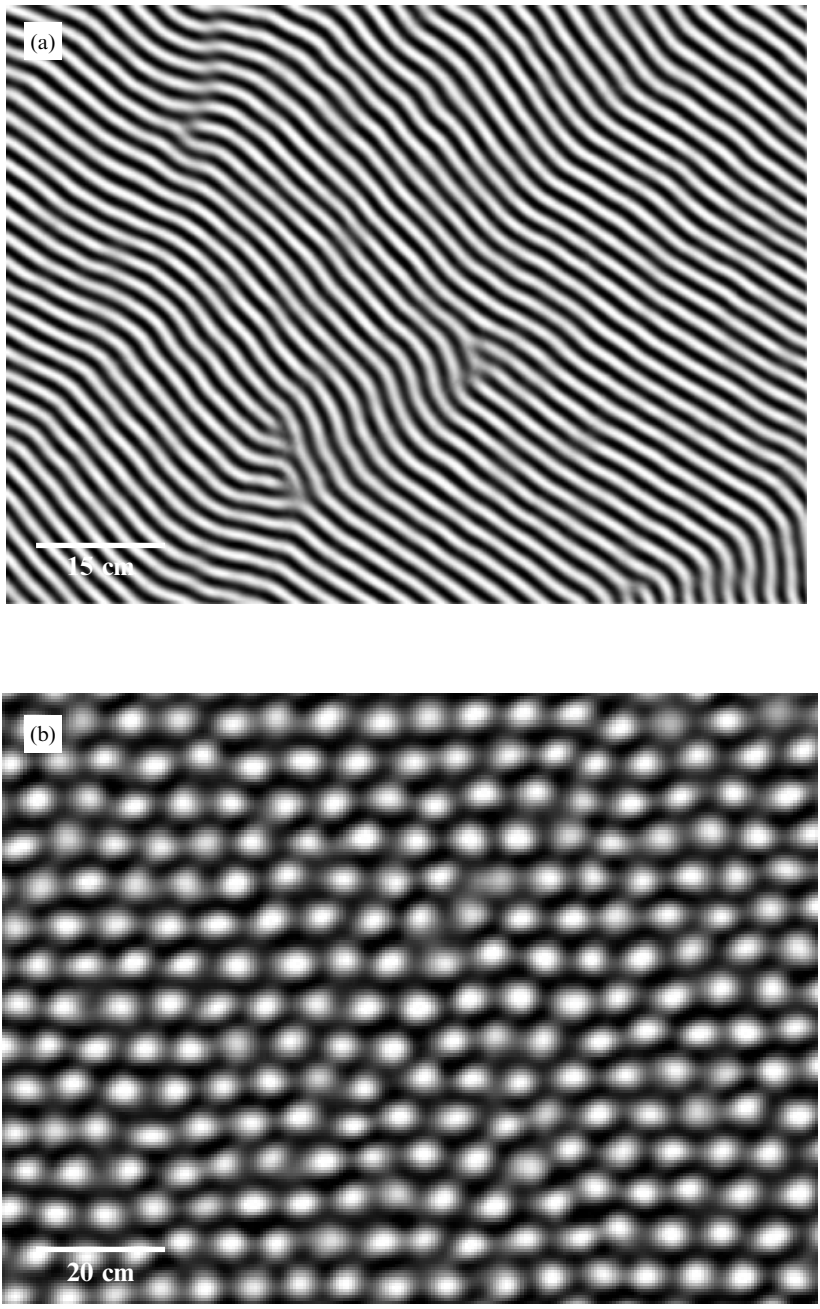

Figure 9.2 Panels (a), (b) show representative SEM images of cylinders and spheres, respectively. These images can be interpreted as plan views of the corresponding panels of Figure 9.1. Bar = 100 nm.

the matrix (hard and soft) is sufficient to give rise to contrast in PS-PEP systems [18]. These researchers have argued that there is virtually no topography in their samples and that the tip taps through a wetting layer of the softer material to sense the harder microdomains. However, contrast may originate from an entirely different mechanism: polymer–tip interactions that strongly depend upon the polymer chemistry. Lastly, it should be pointed out that it is always difficult to completely decouple any one of these effects from the others without extremely careful experiments [28,30].

9.4 MECHANISMS TO CONTROL ORIENTATION

Control over the alignment of microdomains in block copolymer films greatly increases their utility for lithography. For example, if spherical microdomains were arranged onto a lattice and modified to form metal nanodots, in theory each one could function as an addressable memory bit at a density of 10^{11} per square centimeter. Similar arguments for cylindrical microdomains suitably modified to form wires suggest that circuitry could be fabricated if only orientational control could be imposed. With these goals in mind, much effort has been made to control the orientation of films cast from copolymer solutions. The surface imposed by a flat interface (i.e. silicon wafer) does strongly affect the microdomains orientation, but the resulting orientation is not typically desirable. For example, symmetric copolymers that form lamellae usually orient with their planes parallel to the wafer interfaces, thereby reducing their utility as lithographic templates (Figure 9.1c). In an analogous fashion, cylindrical microdomains in thin films typically orient parallel to the wafer plane, but their in-plane orientation varies throughout the film. In what follows, we discuss techniques that have been exploited to control microdomain orientation with an eye towards optimizing a lithographic template.

9.4.1 ORIENTATION CONTROL THROUGH MICROFABRICATION OF TEMPLATES

Perhaps the simplest manner in which to control the orientation of microdomains is to impose physical or chemical topography. Until the last year or so, most efforts in this field had been largely restricted to influencing the features of polymer islands on topographically or chemically patterned substrates. Heier and coworkers [31,32] demonstrated that periodic chemical patterning influenced the local thickness of polymer films subsequently applied. They also demonstrated that a moderate degree of lamellar orientation can be achieved with chemically patterned substrates. Nealey and coworkers [33–35] have used an approach where advanced lithography techniques are used to alter the chemistry of the surface layer in a periodic fashion, thereby influencing the

microdomain orientation of subsequently applied layers. Additionally, it has been shown that patterned substrate topography can be used to manipulate the morphology of block copolymer films, such as islands that adopt an anti-conformal arrangement with respect to surface topography [36–38]. While this has led to interesting scientific questions, control of cylindrical or spherical microdomain orientation is the most challenging and most rewarding goal.

Segalman *et al*. [39] have recently demonstrated that arrays of microfabricated mesas can be used to template PS-P2VP microdomains. Micrometer-scale structures were fabricated on silicon wafers and copolymers were subsequently applied via spin coating. These researchers found that the step edge could be used to template the edge of a single layer of microdomains, and hence the microdomain lattice itself (Figure 9.3). Interestingly enough, there is a slight difference in angle between the step and the microdomain lattice. Sibener and coworkers [40] have also begun to demonstrate control in a similar fashion with a PS-PMMA system. Such work is very exciting because it forwards a means of microdomain control, a crucial enabler of copolymer lithography.

The authors have demonstrated an analogous, though surprisingly different alignment mechanism (Figure 9.4). Silicon wafers were photolithographically patterned with a wide variety of mesas and trenches (typically $4 \times 50\,\mu$m) and a copolymer was applied via spin coating at an average thickness of 30 nm. Highly elongated islands consisting of one layer of cylinders (PS microdomains in a PEP matrix) were observed on the mesas. Surprisingly enough, the islands

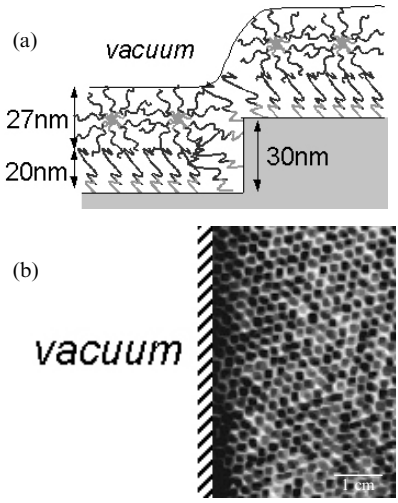

Figure 9.3 (a) Schematic of copolymer chains in the vincinity of a 30 nm step. (b) AFM image of microdomain lattice with lattice orientation templated by mesa edge. Note that microdomains extend to the edge of the step and that the lattice orientation is slightly askew from the step edge. Bar = 150 nm. (Reproduced from R. A. Seyalman *et al. Adr. Mater*. **12**, 1152 (2001), Copyright (2001) with permission from Witey – VCH).

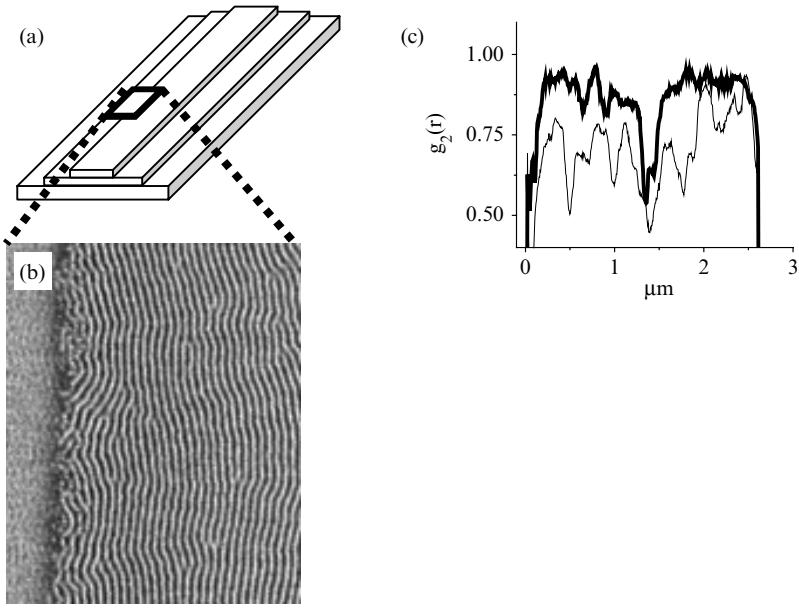

Figure 9.4 (a) Copolymer island (top structure) on silicon mesa (middle structure) fabricated on silicon wafer (bottom). Mesas are typically fifty micrometers long by four micrometers wide, copolymer film is close to three micrometers wide. (b) After spin coating the copolymer film retracts from the mesa edge during annealing and the microdomains orient along the longer dimension of the island. Bar = 200 nm. (c) Plot of microdomain alignment with mesa edge as a function of distance from mesa edge. $g_2(r)$ is the cross-correlation function of the microdomain alignment with the mesa edge where a value of 1.0 indicates perfect alignment. Note that the plot range almost spans the three-micrometer width of the copolymer island of panel (a). The middle of the mesa corresponds to 1.5 micrometers on the graph. At early times (thin line) $g_2(r)$ varies between 0.5 to 0.75, reflecting the poor alignment of the microdomains. At later times (thick line) the microdomains become more aligned and $g_2(r)$ is closer to 1.0 except for a misalignment region in the middle of the mesa. This region (dip on the graph at 1.5 micrometers) disappears with further annealing.

extended along the length of the mesas but the film retracted from the mesa edge. These elongated islands were observed to effectively orient the cylinders over dozens of micrometers, though presumably the alignment length is potentially as long as the wafer.

Cheng *et al*. [41] have recently demonstrated that the spherical microdomains of a polystyrene-polyferrocenyldimethylsilane (PS-PFS) block copolymer can be templated by microfabricated grooves. In this case the topographic relief structures were microfabricated by interference lithography, though presumably conventional lithographic techniques would work as well if high resolution was obtained. These authors demonstrated that microdomains subsequently applied aligned with grooves and that the ordering proceeded from the walls inward. Furthermore, they were able to use these microdomains to fabricate

silica posts by reactive ion etching. Presumably this technique could be extended to fabricate an array of W-Co dots as well.

Hot-stage AFM is being used to investigate the kinetics of microdomain alignment with respect to a microfabricated step edge [26,42]. There has been some evidence that the alignment near a step edge proceeds faster than the coarsening process in the absence of a step. The results here are especially pertinent to the use of microfabricated steps to align microdomains. Defects may be repelled or absorbed by the step; one may be able to analyze this motion in an analogous fashion to the motion of image charges. Cheng and coworkers [41] have confirmed these observations by pointing out that PS-PFS microdomains in grooves align first at the outside and the alignment proceeds towards the middle.

Finally, it has been shown that the trenches formed by embossing – a much cheaper process than microlithography – can be used to control the lattice orientation of spherical microdomains for the purposes of information storage (see Section 9.7) [43,44]. A thorough understanding of the alignment process would provide insight into the use of any one of the techniques mentioned in this section.

9.4.2 ELECTRIC FIELDS

It has been shown that electric fields can be used to align polymeric microdomains, typically by taking advantage of the mismatch of the dielectric constants of two or more blocks. Amundson and coworkers [45–47] demonstrated the effectiveness of such techniques in a bulk PS-PMMA system where the respective dielectric constants are listed as 2.55 and 3.78, evidently sufficient for macroscopic alignment. Birefringence analysis was performed to show that the order parameter, a measure of the degree of field alignment, grew with time upon application of fields in the range of 15 kV per cm until saturation. Additionally, defect analysis was performed to correlate the birefringence data with electron microscopy images.

There have been two main techniques for electric-field alignment in thin films: in-plane and out-of-plane electrodes. The potential of microfabricated in-plane electrodes has been elegantly demonstrated by Morkved *et al*. [48] who showed that sufficiently strong electric field fields could be generated to align cylindrical microdomains (Figure 9.5). Though these researchers worked with a kinetically hindered PS-PMMA system, impressive alignment was demonstrated by annealing above the glass transition temperature in the presence of an electric field. TEM analysis of such samples was facilitated by sample fabrication on silicon nitride membranes. Unfortunately, the region of microdomain alignment extended only a micrometer or so beyond the metal electrodes. These researchers estimate that 30 kV/cm is necessary to orient the microdomains. While the technique demonstration was beautiful, its ultimate

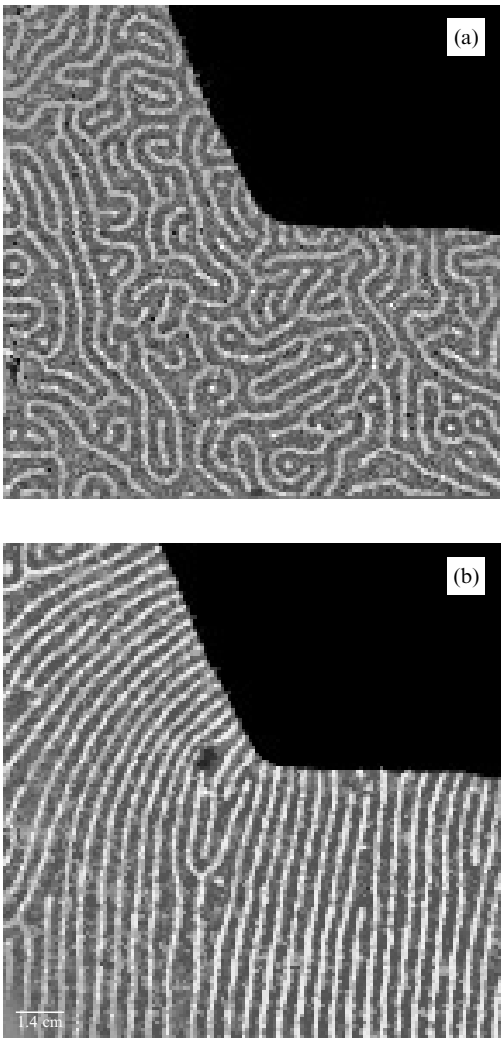

Figure 9.5 (a) AFM image of cylindrical microdomains in the vicinity of an electrode; field has not yet been applied and the average orientation is random. (b) After application of the electric field the microdomains have oriented parallel to the field lines emerging normal to the electrode edge. Bar = 150 nm. (Reproduced from T. L. Morkved *et al. Science* **273**, 931 (1996), copyright (1996) with permission from the American Association for the Advancement of Science).

use as a mean of generating macroscopic microdomain control would be challenging as the entire wafer would need to be patterned with electrodes, a technical challenge.

Thurn-Albrecht *et al.* [49] have shown that out-of-plane electrodes can force cylindrical PS microdomains to orient perpendicular to the substrate in a

PS-PMMA system (Figure 9.6). The alignment field (30 V/μm), produced by metal electrodes above and below the polymer film, acts like a parallel-plate capacitor with a micrometer-scale separation. While this technique is very successful in aligning cylinders perpendicular to the substrate, the field has little or no effect on the packing of the cylinders. A plan view of these structures reveals a polycrystalline lattice-like structure where each grain adopts a random orientation. Furthermore, these researchers have used lithography techniques to erode away PMMA cylinders and back fill with various metals, such as Co

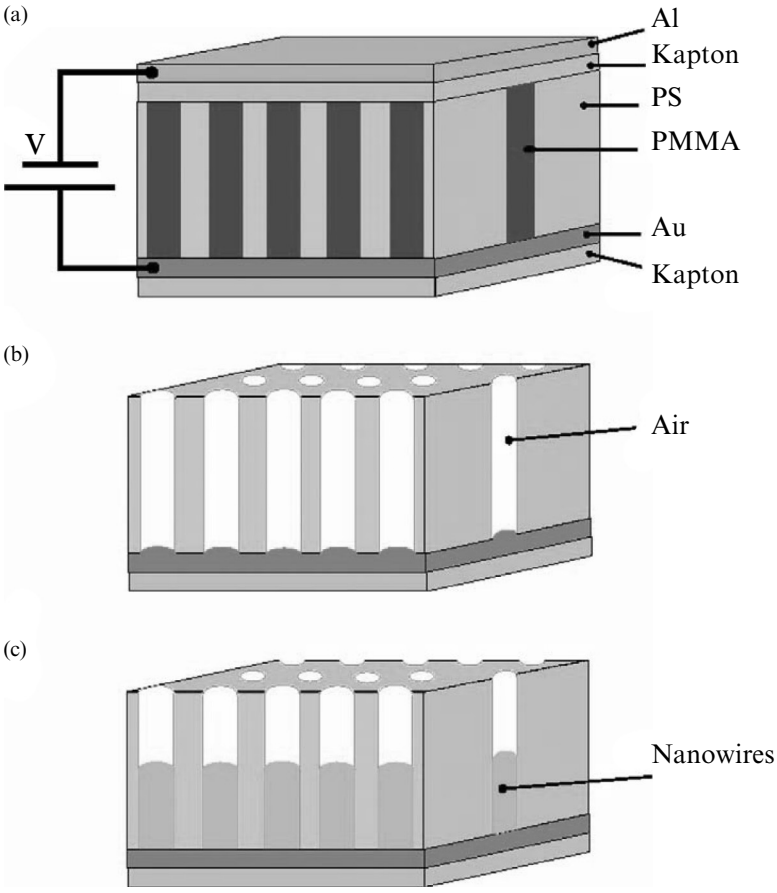

Figure 9.6 Fabrication steps to make an array of nanowires oriented perpendicular to the substrate. (a) The PS-PMMA copolymer forms cylinders oriented perpendicular to the substrate when poled with an electric field above the glass temperature. (b) The oriented PMMA cylinders are removed by exposure to deep ultraviolet light. (c) Co or Cu wires are grown in cylindrical holes by electrodeposition. (Reproduced from T. Thurn-Albrecht *et al. Science*, **290**, 2126 (2000), copyright (2000) with permission from the American Association for the Advancement of Science).

and Cu. Coercivity measurements were performed and found to be rather large, $H_c = 800$ Oe at 300 K. Here, the wire diameter is much smaller than the theoretical critical single-domain behavior (around 50 nm) so that single-domain behavior is possible. These authors suggest that coercivity can be tailored by the aspect ratio of the wires and their packing density. This method shows great promise and is an impressive combination of science and technology.

9.4.3 SHEAR ALIGNMENT

Shear alignment of bulk polymeric samples has been a standard technique for decades and its applicability to block copolymers for the purposes of controlling order has been soundly demonstrated by both Kornfield and Winey [50–54]. Such shearing techniques have been extended to thick polymer films by Albalak and Thomas [55] using counter-rotating cylinders (roll casting). The simplicity of shear alignment is appealing but challenging to utilize on films with thicknesses comparable to that of a microdomain. However, some progress has been made. Typically, a film is cast on a silicon wafer and a second wafer – treated with adhesion-preventing polymers – is pressed on top and held under pressure, usually at an elevated temperature. Chou and coworkers [56] are beginning to investigate the utility of such techniques to align single layers of microdomains for the purposes of microfabrication. This technique necessitates clean-room conditions as any dust particles between the two wafers will prevent adequate contact. One alternative route is to replace the treated wafer with a robust strip of conformal silicone (poly(dimethyl siloxane)). Pressure could be applied to the polymer-coated wafer through the PDMS at moderately high temperatures. A few randomly distributed dust particles would not prevent a large degree of contact between the surfaces. Such techniques may make this technique accessible to a wider range of researchers.

9.4.4 ALIGNING MICRODOMAINS VERTICALLY THROUGH INTERFACE CONTROL

Perhaps the earliest contribution to the control of microdomain orientation via interface control was the experiments of Mansky *et al.* [5], who demonstrated that cylindrical microdomains could be oriented perpendicular to a film by solvent casting on an aqueous surface. It was also demonstrated here that ozone could be used to selectively remove PB microdomains from a PS matrix, thereby enabling subsequent research in lithography. However, the uniformity of this sample preparation method was highly lacking – only certain randomly distributed regions of samples prepared in this manner yielded perpendicularly orinted cylinders.

Building on this work, Huang *et al*. [57,58] have demonstrated that clever tuning of the interfacial energies of thin films can be used to control microdomain orientation in PS-PMMA copolymers. Lamellae were induced to orient perpendicular to a substrate through the use of random copolymers, as demonstrated by both small-angle neutron scattering and electron microscopy. PS-PMMA films were typically cast on surfaces tailored to be neutral to wetting by either block, leading to the perpendicular orientation. Challenges remain, however, in assuring the uniformity of alignment throughout the sample, and increasing the correlation lengths of the microdomains. Perhaps a combination of this technique with alignment-inducing physical topography would be a winning combination.

9.4.5 DIRECTIONAL CRYSTALLIZATION

Temperature gradients are extensively used to grow single-crystal silicon ingots, and their application to polymer microdomains is a natural and intriguing extension. One typically starts with a seed crystal with a well-determined lattice orientation and immerses it into a melt to trigger crystallization. Zone refining (repeated movement of a melting and crystallizing zone) can be exploited to exclude impurities and defects from the region of interest. Bodycomb and Hashimoto [59,60] have applied this methodology to bulk lamellar systems to form well-oriented samples without shear. Further application of this technique to thin films – facilitated by temperature gradient stages – may provide an additional pathway to macroscopic sample orientation [61].

Alternatively, one can directionally solidify a crystallizable material for the purposes of templating the orientation of microdomains. Researchers have shown that benzoic acid can be suitably crystallized and polystyrene-polyethylene diblock copolymers that are dissolved into benzoic acid will form microdomains with an orientation perpendicular to the substrates [62]. While this is very powerful, it not clear that suitable solvents can be found for a wide variety of copolymer systems such that this can be generalized. Additionally, the grain size of the cylinders is very small, so that addressability of the cylinders is rendered difficult.

9.4.6 CONTROL VIA FLUIDICS

Thomas and coworkers [62] have used a novel application of microfluidic technology to begin to control microdomain array orientation. Standard soft lithography techniques were used to fabricate microfluidic channels out of poly (dimethyl siloxane) (PDMS) that were placed onto a semiconductor wafer [63]. Polymer solutions were allowed to flow into the channels and the solvent

evaporated, resulting in microdomains in controlled areas of the wafer [64]. At present, little control of the microdomain patterns has been demonstrated, but this technique has great potential to place polymer films in specific areas of a wafer, a useful addition for high-throughput measurements.

9.4.7 EMBOSSING

Perhaps the simplest, yet most effective method for templating microdomain orientation is with physical embossing, such as in the manufacturing of compact discs. For this process a hard master with relief structures is manufactured. The platter to be embossed is coated with a relatively deformable material, such as a resist. The resist to be embossed is coated with a "nonstick" surface, such as chemical species with fluorine groups. Copolymer films can be spin coated onto such grooved surfaces to template the location of copolymer microdomains [56]. Koji and coworkers have successfully used this templating methodology for information technology (Section 9.7).

9.5 METALLIC INCOPORATION OR MODIFICATIONS TO THE COPOLYMER TEMPLATE

For the purposes of patterning media such as silicon wafers, differentiation of the microdomains is often desirable. For many systems, both copolymer blocks are carbonaceous, leading to an etch resistance between the microdomains and the matrix that is less than desirable (see Section 9.6). However, this can be differentiated by for example, incorporating metal clusters into one block. In what follows we describe suitable modification schemes.

9.5.1 METAL INCORPORATION VIA EVAPORATION

The simplest means to template the placement of metal is to evaporate it onto the proper choice of a copolymer film. For those copolymer blocks with sufficiently disparate metal–polymer interactions, interfacial energies can be used to tailor the ultimate location of metallic particles after coalescence. Segregation of metals into microdomains have been demonstrated in this manner by Jaeger and coworkers [65,66]. While only a limited set of metals satisfy the constraints, metal films so fabricated would act as robust masks (Figure 9.7). Most interestingly, chains of such segregated particles lead to fascinating transport properties.

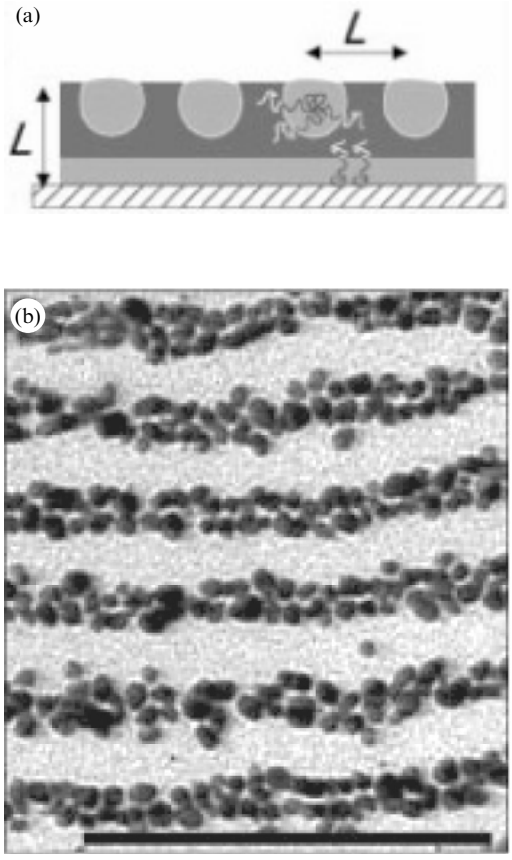

Figure 9.7 (a) Schematic of PS-PMMA in thin film, where both PS and PMMA component are exposed to free surface. (b) Evaporated gold on copolymer template, followed by annealing leads to segregation with cylinder loading fractions up to 30 %. Bar = 250 nm. (Reproduced from W. A. Lopes and H. M. Jaeger, *Nature*, **414**, 735 (2001), copyright (2001) with permission from Nature Publishing Group).

9.5.2 METAL INCORPORATION VIA DIRECT SYNTHESIS

Cohen and coworkers [67–69] have made strong contributions to the field of block copolymers by directly synthesizing metal nanoclusters in copolymer materials. Starting with organometallic monomers, a variety of processing means, such as heating or reduction with hydrogen have been employed to convert the metal atoms to clusters. These researchers have demonstrated the fabrication of silver, platinum, copper, nickel, and gold nanoclusters. The metal clusters follow the block copolymer microdomain templates to varying degrees, with perhaps the greatest success with silver. These techniques have the possi-

bility of fabricating microdomains with ultimate etch resistance as many metals are not attacked by reactive ion etching. One disadvantage, however, is that the metal clusters rarely occupy more than half the microdomain volume, minimizing the effectiveness of a microdomain mask. Generating continuous metal lines in the form of cylinders remains a challenge.

Spatz *et al.* [70] have made large contributions to the field of nanoparticle patterning through the development of successful gold particle fabrication schemes and extensive characterization. Ultrathin films of PS-P2VP are typically applied to substrates by dip coating mica substrates into a micellar solution. Films are created with an average thickness less than 10 nm (Figure 9.8). Favorable interactions between PS and titanium resulted in preferential deposition of evaporated titanium onto PS domains, thereby dramatically increasing their etch resistance. Control of the spacing, though not the resulting microdomain order, was demonstrated. Argon ion milling was then used to transfer the pattern into the gallium arsenide substrate. An alternative approach was demonstrated as well, whereby PS-P2VP micelles were formed in solution and treated to bind $AuCl_4$ ions to the micelle cores. Reduced gold particles inside micelles that are transferred to a substrate act as the lithographic mask into gallium arsenide [71]. Whether any of these processes lead to patterned GaAs with quantum-dot-like characteristics has yet to be shown. Such processes, unfortunately, lead to many crystal defects, preventing the fabrication of quantum dots.

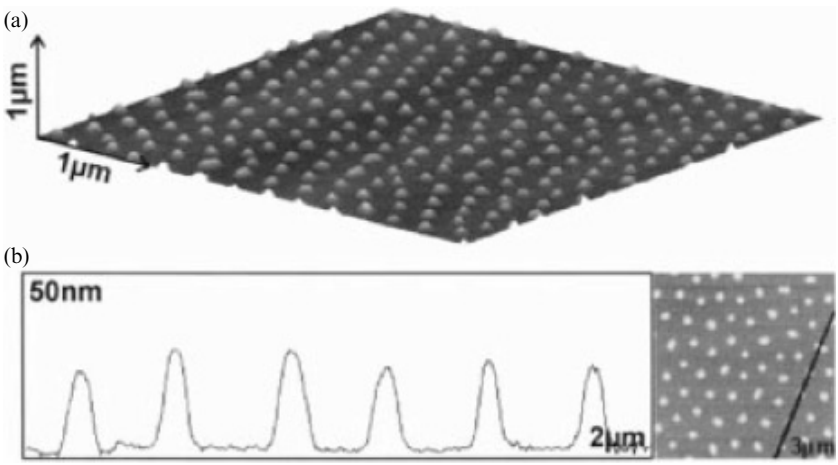

Figure 9.8 (a) AFM image of a layer of micelles formed in a solution of PS-P2VP and applied to mica. A layer of Ti/TiO_2 was subsequently applied and the micelle height increased, indicating a segregation of the evaporated coating. (b) Height profile of AFM image indicating 27 nm corrugation height. (Reproduced from J. P. Spatz *et al. Adv. Mater.*, **10**, 849 (1998), copyright (1998) with permission from Wiley–VCH).

9.6 LITHOGRAPHIC USE OF TEMPLATES

In this section we focus on the patterning of materials by copolymer templates. Building on the film preparations of Section 9.5 we discuss chemical-based wet-etching processes and plasma-based dry-patterning techniques. Ensuring the compatibility of copolymer etching steps with commonly used processes is advantageous as it should speed industrial adoption of this technology. We highlight two successful copolymer templating processes – ozonated PS-PI films and polyisoprene-polyferrocenyldimethylsilane.

9.6.1 PATTERN TRANSFER METHODOLOGIES: WET AND DRY

Perhaps the simplest and oldest pattern transfer technique is wet etching, which is surprisingly effective even for copolymer templates. Typical use of wet etching involves photolithography or electron beam lithography to selectively expose substrate areas for dissolution. An aggressive liquid etchant is then used to remove exposed areas of a wafer. One historical drawback has been the isotropic nature of many etchants so that high aspect features are difficult to fabricate. However, as will be discussed in Section 9.6, some success has been reported for copolymer templates.

Dry-etching processes such as reactive ion etching (RIE) and plasma etching are the dominant tools for pattern transfer of submicrometer features. A pattern is generated on a resist-coated wafer and this pattern is transferred by a directed plasma of high-energy ions. Plasmas typically consist of gases of CF_4, O_2, SF_6, Cl_2, or argon. Etching takes place by a combination of physical bombardment (sputtering) and chemical reactivity to make volatile compounds. Copolymer lithography was initially demonstrated with a low-power, low-pressure CF_4 plasma using a PS-PI system. Low-pressure etching conditions were used to maximize the average path length of the ions so as to facilitate anisotropic etching [72,73].

9.6.2 PATTERNING VIA AN OZONATED COPOLYMER TEMPLATE

The earliest patterning techniques took advantage of ozonation to dissolve microdomains away from the matrix, leaving a single array of pores in a thin film. This porous film then acted as a standard etching mask, where the pores presented less etch resistance than the matrix. CF_4-based RIE was shown to be the most effective tool in pattern transfer from the thin film to the substrate. It was first demonstrated that standard semiconductor materials – such as silicon or silicon nitride – could be easily and uniformly patterned by this technique [5,72,73]. Starting with a copolymer-coated silicon wafer, an hexagonal array of holes with a 20 nm depth and a 40 nm lattice constant was uniformly etched into the sample (Figure 9.9). These researchers were

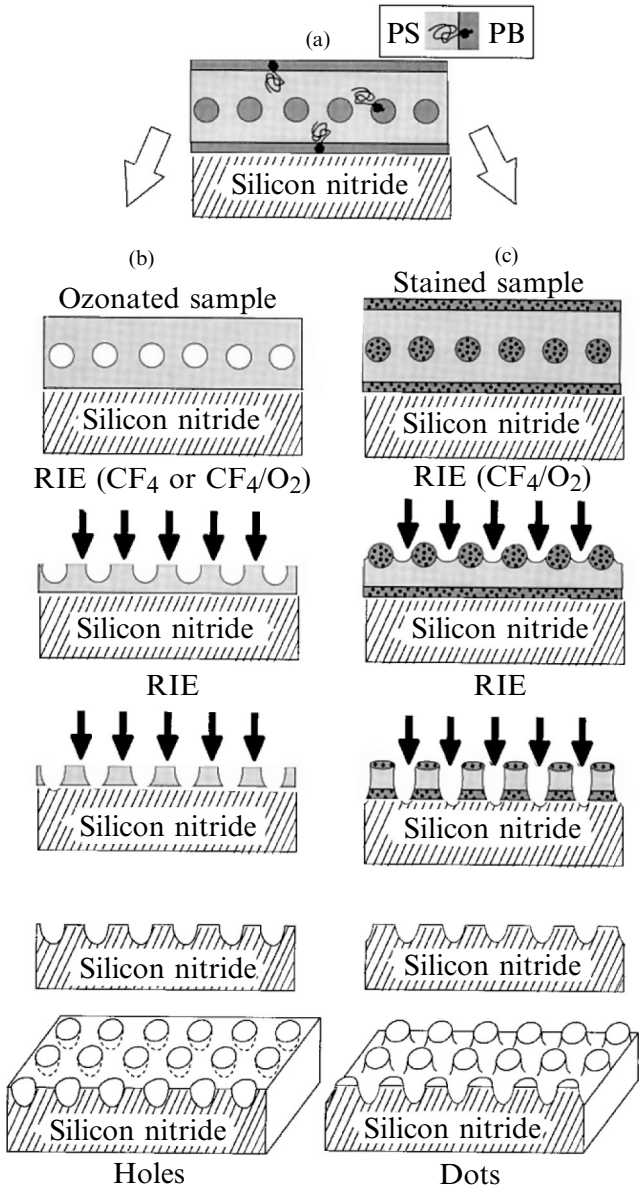

Figure 9.9 Two complementary fabrication strategies used by Chaikin and coworkers to pattern substrates. The left side shows the removal of microdomains by ozonation, thereby acting as a positive resist. The right side shows the crosslinking of microdomains by staining, thereby acting as a negative resist. In both cases reactive ion etching is used to transfer the template to the substrate. The two processes are used to fabricate holes or dots, respectively. (Reproduced from M. Park *et al. Science*, **278**, 1401 (1997), copyright (1997) with permission from the American Association for the Advancement of Science).

challenged to fabricate deeper holes as the polymer film matrix presented little etch resistance. This technique was further extended to fabricate an array of gold dots via a boot-strapping trilevel procedure. Wafers were coated with a thin layer of polyimide and then coated with an even thinner film of silicon nitride via plasma-enhanced chemical vapor deposition. A single layer of copolymer microdomains was applied via spin coating. After appropriate annealing and ozonation, the copolymer film was used to pattern through the silicon nitride via CF_4 RIE. Using the silicon nitride film as a mask, O_2 RIE was used to pattern cylindrical holes down to the silicon wafer, onto which gold was evaporated. The polyimide was dissolved away, leaving an array of gold dots on the wafer [74]. The ultimate goal of these researchers is two-fold; primarily they are interested in the electron-transport properties of patterned metal films, but additionally the possibilities for information storage (one bit per dot) are lucrative [75]. Further extension of this technique includes the fabrication of metal wires using a template of cylindrical microdomains.

Li *et al.* [76] were able to employ ozonation technologies to pattern GaAs substrates using a copolymer template and a combination of wet- and dry-etching technologies. The ultimate goal of this project is to generate quantum dots with a tighter size distribution than currently possible via Stranski–Krastanow growth or metal-organic chemical vapor deposition [77,78]. Starting with a copolymer-coated GaAs wafer, the microdomains were dissolved away and the films were plasma etched, generating topographical contrast. Wet etching (mixture of ammonium hydroxide and hydrogen peroxide) was used to transfer the pattern into GaAs with both the (100) and (311)B orientation. As wet etching is often more gentle than direct reactive ion etching, this technique may play a role where disruption of the crystal lattice is not acceptable.

9.6.3 PATTERNING VIA PI-PFS COPOLYMER TEMPLATE

Thomas and coworkers [41,79–82] have demonstrated that a polyisoprene-polyferrocenyldimethylsilane (PI-PFS) copolymer is a more robust mask as compared to purely organic copolymers. The ferrous component – which formed the microdomains – was demonstrated to be strongly resistant to an oxygen-based plasma. Metal is incorporated directly during polymerization rather than subsequent modifications to the template. Etch-resistance ratios as high as 50 were reported for the organic vs ferrous material for an oxygen plasma. In one demonstration, a boot-strapping process was used where PI-PFS was used to pattern silicon oxide via oxygen-based RIE, the patterned silion oxide was used to mask tungsten for etching via CHF_3, and finally the patterned tungsten film was used to pattern a cobalt film. Optimal choice of the etching gas and conditions used at each step led to optimal patterning (Figure 9.10). These researchers showed that the coercivity increased as a function of etch depth; arrays of individual dots had a higher coercivity than a continuous

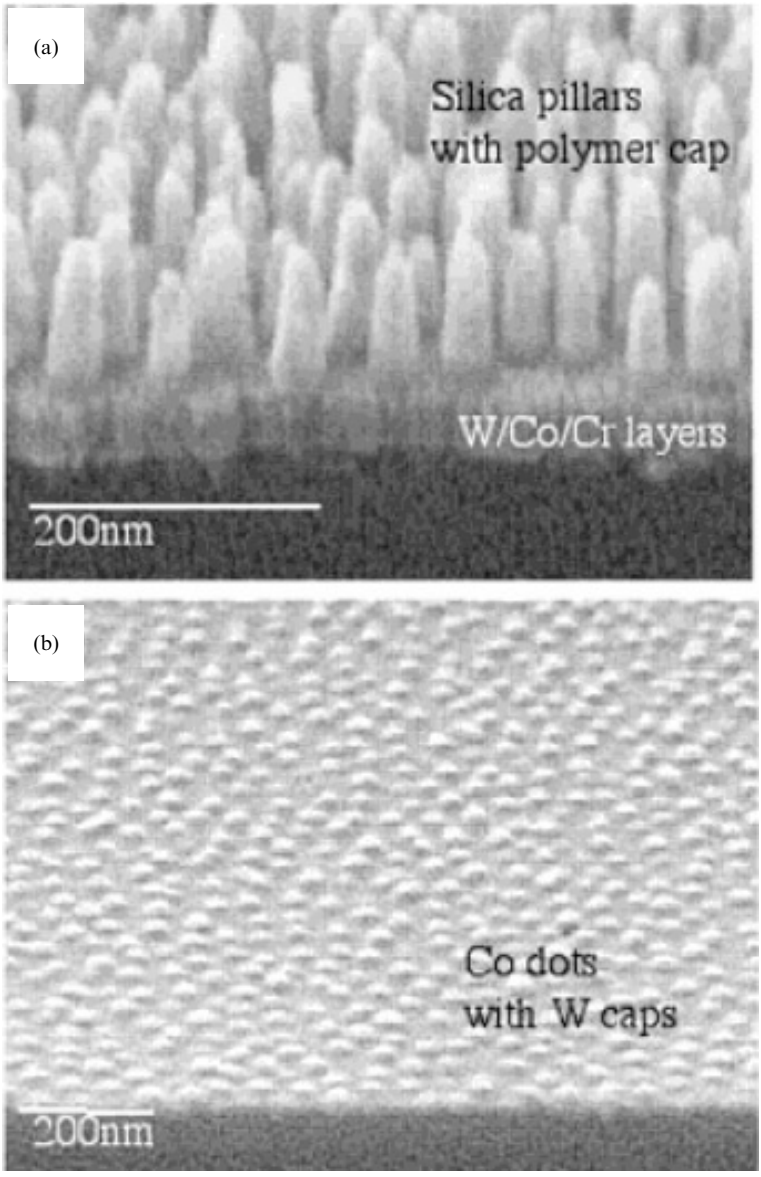

Figure 9.10 Fabrication strategy used by Thomas and coworkers. (a) Pillars of silicon oxide topped with oxidized PFS after etching with CHF_3 based RIE. (b) Tungsten-topped cobalt dots produced as final product. Bar = 200 nm. (Reproduced from J. Y. Cheng *et al*. *Adv. Mater*. **13**, 1174 (2001) copyright (2001) with permission from Wiley-VCH).

film. The authors argued that domain-wall motion, necessary to switch magnetization direction, was impeded by defects introduced by etching.

9.6.4 PATTERNING VIA PS-PMMA COPOLYMER TEMPLATE

PS-PMMA systems can be used as lithographic templates in a similar manner to PS-PI systems but with a different degradation mechanism. PMMA degrades quickly when exposed to ultraviolet light and can then be washed away. Therefore, after fabrication of a thin film of PS-PMMA microdomains, the PMMA can be degraded and removed, producing a matrix of voids. These can then be used as a lithographic template for the purposes of masking a wafer or filling with metal [49]. Alternatively, PMMA is less resistant to dry etching with an oxygen plasma, providing an additional route to patterning (further discussed in Section 9.7).

9.7 CURRENT APPLICATIONS OF BLOCK COPOLYMER LITHOGRAPHY

Asakawa and coworkers [43] have demonstrated that PS-PMMA copolymer films can be used for patterning magnetic media for information storage. Copolymers consisting of PS and PMMA have the advantage of being both controllable by an electric field and also having etch-rate ratios of at least a factor of two under CF_4-based dry etching. Taking advantage of the latter, these researchers developed a three-step etching process whereby PS-PMMA patterns could be directly transferred to 6.26 cm (2.5 inch) glass disks designed for hard-drive applications. A metal film was sputtered onto the glass disk consisting of Ti (adhesion promoter) followed by $Co_{74}Pt_{26}$, the magnetic layer for information storage. A novolac-based resist was then spin coated onto this for embossing. A nickel master with spiral relief structures was used to imprint the novalac resist disk where the spiral widths ranged from 60 to 250 nm (Figure 9.11) [43]. The spiral pattern was transferred to the disk at a pressure of 1000 bar resulting in spiral grooves. A PS-PMMA diblock copolymer solution was spin coated onto this patterned disk and annealed, inducing microdomains to cluster in the lines. While the ordering of the dots along the grooves is not extremely regular (as is often the case with PS-PMMA systems), they are well defined and appear undamaged from this process. A modification of the above process was undertaken as well – after oxygen etching to remove the PMMA microdomains, spin-on glass (SOG) was applied that selectively filled the holes. Ion milling through the SOG was then used to pattern the underlying metal film. Measurements revealed that the coercivity of such films increased as compared to the continuous film. These researchers used magnetic force microscopy to demonstrate that the media could be erased by DC magnetic fields.

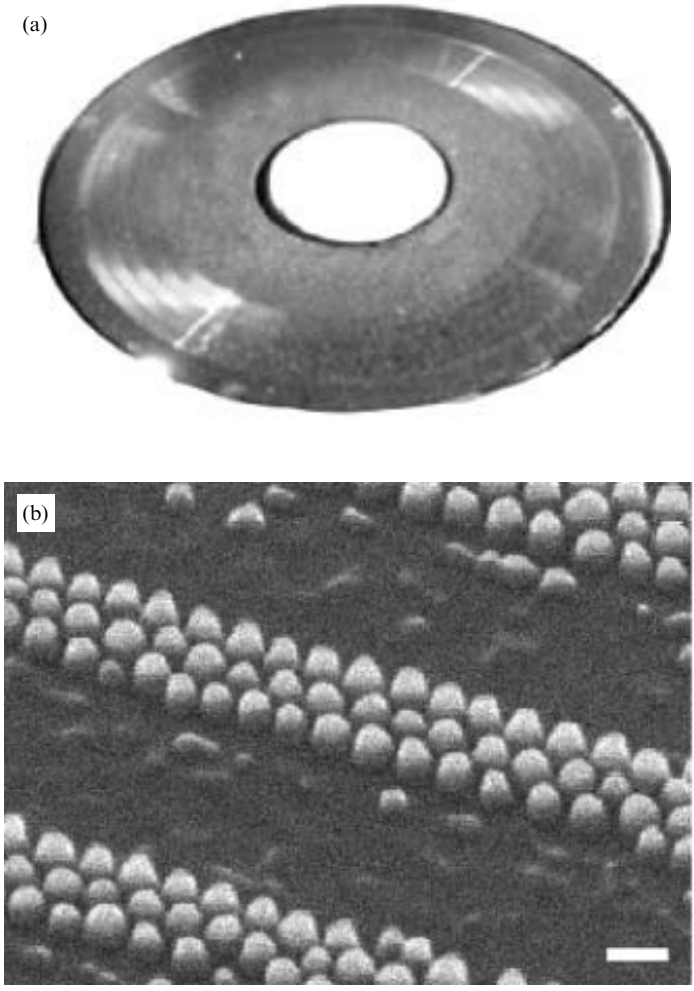

Figure 9.11 Fabrication strategy employed by researchers at Toshiba. (a) 6.25 cm (2.5 inch) HDD glass plate used for information storage. Circular lines originate from interference colors of embossed lines. (b) SEM micrograph of CoCrPt dots formed from copolymer template in substrate grooves. Bar = 50 nm. (Reproduced from K. Asakawa *et al. J. Photopolym. Sci. Technol*, **15**, 465 (2002) copyright (2002) with permission from J. Photopolym. Sci. Technol).

9.8 SUMMARY AND FUTURE DIRECTIONS

During the past decade, research on copolymer lithography began as a trickle and has now increased to a torrent. The elementary patterning techniques first demonstrated by Chaikin and Register have been further developed by the

techniques of the research groups of Thomas, Kramer, and Russell. It is soundly demonstrated that there are multiple paths to taking a self-assembled copolymer pattern with a 20 nm feature size and transferring it to a semiconductor or metallic substrate. Unfortunately, it has yet to be demonstrated that an entire hexagonal array of metal dots can be generated with lattice-like registry. However, as Asawaka and coworkers have shown, there may be alternative paths to information storage that do not require such registry. A combination of the emerging orientation control techniques and the patterning technologies of copolymer systems such as PI-PFS should prove to be a winning combination.

Lastly, researchers who are able to take the long view realize that the techniques and insight developed here may best come to fruition with a self-assembling system that is not based on copolymers. For example, applications may emerge more quickly with silicates templated by surfactants than with self-assembling copolymers. Even so, it is doubtless that the techniques and processes developed for copolymer lithography will assist researchers in these fields as well.

ACKNOWLEDGEMENTS

CH thanks Ian Hamley for the opportunity to write this review and cheerfully acknowledges fruitful discussions with Michael Fasolka. CH has unlimited gratitude to his advisors at Princeton – Paul, Rick, and David – whose amazing degree of intelligence and patience never ceases to astound him. JAD acknowledges support by the NIST Office of Microelectronics Programs for portions of this work.

REFERENCES

1. C. Y. Chang and S. M. Sze, *ULSI Technology*. McGraw-Hill Higher Education, New York, 2 edition, 1996.
2. M. J. Fasolka and A. M. Mayes, *Ann. Rev. Mater.*, **31**:323, 2001.
3. P. M. Chaikin, personal communication.
4. D. Hofstadter, *Phys. Rev. B*, **14**:2239, 1976.
5. P. Mansky, P. M. Chaikin, and E. L. Thomas, *J. Mater. Sci.*, **30**:1987, 1995.
6. Certain commercial equipment, instruments, or materials are identified in this chapter in order to specify the experimental procedure adequately. Such identification is not intended to imply recommendation or endorsement by the National Institute of Standards and Technology, nor is it intended to imply that the materials or equipment identified are necessarily the best available for the purpose.
7. C. T. Kresge, M. E. Leonowicz, W. J. Roth, J. C. Vartuli, and J. S. Beck, *Nature*, **359**:710, 1992.
8. W. B. Russel, D. A. Saville, and W. R. Schowalter. *Colloidal Dispersions*. Cambridge University Press, New York, 1992.

9. F. S. Bates, *Science*, **251**:898, 1991.
10. F. S. Bates and G. H. Fredrickson, *Annu. Rev. Phys. Chem*., **41**:525, 1990.
11. L. J. Fetters, D. J. Lohse, D. Richter, T. A. Witten, and A. Zirkel, *Macromolecules*, **27**:4639, 1994.
12. R. P. Quirk and L. J. Fetters, *Comprehensive Poymer Science*, volume 7, chapter 1, page 1. Pergamon Press, 1989.
13. K. A. Davis and K. Matyjaszewski, *Adv. Polym. Sci*., **159**:1, 2002.
14. D. Bendejacq, V. Ponsinet, M. Joanicot, Y. L. Loo, and R. A. Register, *Macromolecules*, **35**:6645, 2002.
15. K. Matyjaszewski, *Controlled Living Radical Polymerization: Progress in ATRP, NMP, and RAFT*, volume 768. American Chemical Society, Washington D.C., 2 edition, 2000.
16. K. Matyjaszewski and J. Xia, *Chem. Rev*., **101**:2921–2990, 2001.
17. C. J. Hawker, A. W. Bosman, and E. Harth, *Chem. Rev*., **101**:3661–3688, 2001.
18. C. Harrison, Z. D. Cheng, S. Sethuraman, D. A. Huse, P. M. Chaikin, D. A. Vega, J. M. Sebastian, R. A. Register, and D. H. Adamson *Phys. Rev. E*, **66**:011706, 2002.
19. C. S. Henkee, E. L. Thomas, and L. J. Fetters. *J. Mater. Sci*., **23**:1685–1694, 1988.
20. C. Harrison, P. M. Chaikin, D. A. Huse, R. A. Register, D. H. Adamson, A. Daniel, E. Huang, P. Mansky, T. P. Russell, C. J. Hawker, D. A. Egolf, I. V. Melnikov, and E. Bodenschatz, *Macromolecules*, **33**:857, 2000.
21. A. E. Ribbe, J. Bodycomb, and T. Hashimoto. *Macromolecules*, **32**:3154, 1999.
22. T. L. Morkved, W. A. Lopes, J. Hahm, S. J. Sibener, and H. M. Jaeger *Polymer*, **39**:3871, 1998.
23. D. W. Schwark, D. L. Vezie, J. R. Reffner, and E. L. Thomas, *J. Mater. Sci. Lett*., **11**:352, 1992.
24. C. Harrison, M. Park, P. M. Chaikin, R. A. Register, D. H. Adamson, and N. Yao, *Polymer*, **30**:2733, 1998.
25. C. K. Harrison, M. Park, P. M. Chaikin, R. A. Register, and D. H. Adamson, *Macromolecules*, **31**:2185, 1998.
26. M. L. Trawick, D. E. Angelescu, P. M. Chaikin, M. J. Valenti, and R. A. Register, *Rev. Sci. Instrum*., submitted.
27. B. K. Annis, D. W. Schwark, J. R. Reffner, E. L. Thomas, and B. Wunderlich, *Makromol. Chem*., **193**:2589, 1992.
28. R. G. Winkler, J. P. Spatz, S. Sheiko, M. Moller, P. Reineker, and O. Marti, *Phys. Rev. B*. **54**:8908, 1996.
29. A. Knoll, R. Magerle, and G. Krausch. *Macromolecules*, **34**:4159, 2001.
30. J. P. Spatz, S. Sheiko, M. Moller, R. G. WInkler, P. Reineker, and O. Marti, *Nanotechnology*, **6**:40, 1995.
31. J. Heier, J. Genzer, E. J. Kramer, F. S. Bates, S. Walheim, and G. Krausch, *J. Chem. Phys*., **111**:11101, 1999.
32. J. Heier, E. J. Kramer, S. Walheim, and G. Krausch, *Macromolecules*, **30**:6610, 1997.
33. R. D. Peters, X. M. Yang, Q. Wang, J. J. de Pablo, and P. F. Nealey, *J. Vac. Sci. Technol. B*, **18**: 3530, 2000.
34. R. D. Peters, X. M. Yang, and P. F. Nealey. *Macromolecules*, **35**:1822, 2002.
35. X. M. Yang, R. D. Peters, P. F. Nealey, H. H. Solak, and F. Cerrina, *Macromolecules*, **33**:9575, 200.
36. Z. Li, S. Qu, M. H. Rafailovich, J. Sokolov, M. Tolan, M. S. Turner, J. Wang, S. A. Scharz, H. Lorenz, and J. P. Kotthaus, *Macromolecules*, **30**:8410, 1997.
37. M. J. Fasolka, T. A. Germer, and A. Karim. *Langmuir*. in preparation.
38. M. J. Fasolka, P. Banerjee, A. M. Mayes, G. Pickett, and A. C. Balazs, *Macromolecules*, **33**:5702, 2000.

39. R. A. Segalman, H. Yokoyama, and E. J. Kramer, *Adv. Mater*., **12**:1152, 2001.
40. D. Sundrani and S. J. Sibener, *Macromolecules*, **35**:8531, 2002.
41. J. Y. Cheng, C. A. Ross, E. L. Thomas, H. I. Smith, and G. J. Vancso, *Appl. Phys. Lett*. **81**:3657, 2002.
42. M. L. Trawick, M. Megens, C. Harrison, D. E. Angelescu, D. A. Vega, P. M. Chaikin, R. A. Register, and D. H. Adamson, *Scanning*, submitted.
43. K. Asakawa, T. Hiraoka, H. Hieda, M. Sakurai, Y. Kamata, and K. Naito, *J. Photopolym. Sci. Technol*., **15**:465, 2002.
44. K. Naito, H. Hieda, M. Sakurai, Y. Kamata, and K. Asakawa, *IEEE Trans. Magn*. **38**:1949, 2002.
45. K. Amundson, E. Helfand, Xina Quan, S. Hudson, and S. D. Smith, *Macromolecules*, **27**:6559–6570, 1994.
46. K. Amundson, E. Helfand, Xina Quan, and S. D. Smith, *Macromolecules*, **26**:2698–2703, 1993.
47. K. Amundson and E. Helfand, *Macromolecules*, **26**:1324–1332, 1993.
48. T. L. Morkved, M. Lu, A. M. Urbas, E. E. Ehrichs, H. M. Jaeger, P. Mansky, and T. P. Russell, *Science*, **273**:931, 1996.
49. T. Thurn-Albrecht, J. Schotter, C. A. Kastle, N. Emley, T. Shibauchi, L. Krusin-Elbaum, K. Guarini, C. T. Black, and M. T. Tuominen, *Science*, **290**:2126, 2000.
50. Z. R. Chen, J. A. Kornfield, S. D. Smith, J. T. Grothaus, and M. M. Satkowski, *Science*, **277**:1248, 1997.
51. D. L. Polis, K. I. Winey, A. J. Ryan, and S. D. Smith *Phys. Rev. Lett*., **83**:2861, 1999.
52. I. W. Hamley, *J. Phys. Condens. Matter*, **13**:R643, 2001.
53. R. H. Colby, *Curr. Opin. Colloid Interfure Sci*., **1**:454, 1996.
54. G. H. Fredrickson and F. S. Bates, *Annu. Rev. Mater. Sci*., **26**:501, 1996.
55. R. J. Albalak and E. L. Thomas, *J. Polym. Sci. Part B: Polym. Phys*., **31**:31, 1993.
56. L. Zhuang, "Controlled Self-Assembly in Homopolymer and Diblock Copolymer", Ph. D. Thesis, Princeton University (2002).
57. E. Huang, T. P. Russell, C. Harrison, P. M. Chaikin, R. A. Register, and C. Hawker, *Macromolecules*, **31**:7641, 1998.
58. E. Huang, P. Mansky, T. P. Russell, C. Harrison, P. M. Chaikin, R. A. Register, C. Hawker, and J. Mays. *Macromolecules*, **33**:80, 2000.
59. T. Hashimoto, J. Bodycomb, Y. Funaki, and K. Kimishima, *Macromolecules*, **32**:952, 1999.
60. J. Bodycomb, Y. Funaki, K. Kimishima, and T. Hashimoto, *Macromolecules*, **32**:2075, 1999.
61. J. Carson Meredith, A. Karim, and E. J. Amis. *Macromolecules*, **33**: 5760, 2000.
62. C. Park, C. De Rosa, and E. L. Thomas. *Macromolecules*, **34**:2602, 2001.
63. E. Kim, Y. N. Xia, and G. M. Whitesides, *Phys. Rev. B*, **376**:581, 1995.
64. T. Deng, Y. Ha, J. Y. Cheng, C. A. Ross, and E. L. Thomas, *Langmuir*, **18**:6719, 2002.
65. T. L. Morkved, P. Wiltzius, H. M. Jaeger, D. G. Grier, and T. A. Witten, *Appl. Phys. Lett*., **64**:422, 1994.
66. W. A. Lopes, and H. M. Jaeger, *Nature*, **414**:735, 2001.
67. Y. Ng, C. Chan, R. R. Schrock, and R. E. Cohen, *Chem. Mater*., **4**:24, 1992.
68. B. H. Sohn and R. E. Cohen, *Acta Polymer*, **47**:340, 1996.
69. R. T. Clay and R. E. Cohen, *Supramolec. Sci*., **2**:183, 1995.
70. J. P. Spatz, P. Eibeck, S. Mosmer, M. Moller, T. Herzog, and P. Ziemann, *Adv. Mater*., **10**:849, 1998.
71. J. P. Spatz, T. Herzog, P. Eibeck, S. Mosmer, P. Ziemann, and M. Moller, *Adv. Mater*., **11**:149, 1999.

72. M. Park, C. Harrison, P. M. Chaikin, R. A. Register, and D. H. Adamson, *Science*, **276**:1401, 1997.
73. C. Harrison, M. Park, P. M. Chaikin, R. A. Register, and D. H. Adamson, *J. Vac. Sci. Technol. B*., **16**:544, 1998.
74. M. Park, P. M. Chaikin, R. A. Register, and D. H. Adamson, *Appl. Phys. Lett*., **79**:257, 2001.
75. C. Harrison, M. Park, R. A. Register, D. H. Adamson, P. Mansky, and P. M. Chaikin. Method of nanoscale patterning and products made thereby, *United States Patent 5948470*, 1999.
76. R. R. Li, P. D. Dapkus, M. E. Thompson, W. G. Jeong, C. K. Harrison, P. M. Chaikin, R. A. Register, and D. H. Adamson, *Appl. Phys. Lett*., **76**:1689, 2000.
77. T. R. Ramachandran, A. Madhukar, I. Mukhametzhanov, R. Heitz, A. Kalburge, Q. Xie, and P. Chen, *J. Vac. Sci. Technol. B*, **16**:1330, 1998.
78. F. Heinrichsdorff, A. Krost, N. Kirstaedter, M. H. Mao, M. Grundmann, D. Bimberg, A. O. Kosogov, and P. Werner. *Jpn. J. Appl. Phys. Part 1-Regular Papers and Short Notes and Review Papers*, **36**:4129, 1997.
79. J. Y. Cheng, C. A. Ross, V. Z. H. Chan, E. L. Thomas, R. G. H. Lammertink, and G. J. Vancso, *Adv. Mater*, **13**:1174, 2001.
80. R. G. H. Lammertink, M. A. Hempenius, V. Z. H. Chan, E. L. Thomas, and G. J. Vancso, *Chem. Mater*., **13**:429, 2001.
81. R. G. H. Lammertink, M. A. Hempenius, J. E. van den Enk, Chan V. Z. H., E. L. Thomas, and G. J. Vancso, *Adv. Mater*., **12**:98, 2000.
82. J. Y. Cheng, C. A. Ross, E. L. Thomas, H. I. Smith, R. G. H. Lammertink, and G. J. Vancso, *IEEE Trans. Magn*., **38**:2541, 2002.